Journal of Volcanology and Geothermal Research 202 (2011) 228–240

Contents lists available at ScienceDirect

Journal of Volcanology and Geothermal Research

journal homepage: www.elsevier.com/locate/jvolgeores

Co-eruptive subsidence at Galeras identified during an InSAR survey of Colombian volcanoes (2006–2009)

M.M. Parks [a,*], J. Biggs [b], T.A. Mather [a], D.M. Pyle [a], F. Amelung [c], M.L. Monsalve [d], L. Narváez Medina [e]

[a] COMET+, Department of Earth Sciences, University of Oxford, Oxford OX1 3AN, UK
[b] COMET+, Department of Earth Sciences, University of Bristol, Bristol BS8 1RJ, UK
[c] Rosenstiel School of Marine and Atmospheric Sciences, University of Miami, Miami, FL 33149, USA
[d] Colombian Institute of Geology and Mining (INGEOMINAS), Bogotá DC, Colombia
[e] Colombian Institute of Geology and Mining (INGEOMINAS), Pasto, Colombia

ARTICLE INFO

Article history:
Received 28 September 2010
Accepted 21 February 2011
Available online 4 March 2011

Keywords:
Galeras
L-band InSAR
deformation
magma chamber

ABSTRACT

Establishing a time series of deformation is one of the keys to understanding and predicting the magmatic behaviour of active volcanoes. Satellite techniques represent an increasingly useful tool for measuring volcanic deformation over timescales spanning days to decades. Colombia contains numerous young or active volcanoes, many of which are inaccessible. We use L-band (23.6 cm wavelength) radar data acquired between 2006 and 2009, to survey 15 active volcanoes along the Colombian segment of the Northern Volcanic Zone. Analysis of 100 interferograms showed that the majority of volcanoes were not deforming. However, independent interferograms display an average subsidence of 3 cm on the northeast flank of Galeras, coinciding with the January 2008 eruption. We combine InSAR, field measurements and source modelling to determine the origin, size and location of the source of subsidence at Galeras. Our results suggest that this signal was caused by deflation of the magma chamber associated with the January 2008 event. Modelling provides insight into the depth to source (~2 km) and a volume change (-6.5×10^5 m^3) which is consistent with that derived from modelling contemporaneous tilts and the volume of material erupted. Previous studies based on various datasets support the existence of a resident/recurring chamber at this location, over a decadal timescale. Our InSAR results corroborate the hypothesis of shallow magma storage beneath Galeras and provide the first piece of evidence that can be linked to a particular eruption.

© 2011 Elsevier B.V. All rights reserved.

1. Introduction

Colombia's active volcanoes pose a significant hazard and challenge for monitoring, with notable recent events including the 1985 eruption at Nevado del Ruiz and the 1993 eruption at Galeras. Due to the inaccessibility of some sites for field-based monitoring and the probable exposure to hazards, Interferometric Synthetic Aperture Radar (InSAR) is ideally suited to make a significant impact on the monitoring and understanding of volcanic activity in Colombia.

InSAR is an established technique that is routinely used to measure changes in surface elevation between repeat passes of a satellite. InSAR has been successfully employed to determine rates of volcanic deformation associated with structural, hydrothermal and magmatic processes. Examples include the co-eruptive subsidence of Okmok volcano, Alaska (Lu and Dzurisin, 2010) and the uplift resulting from a sill intrusion at Eyjafjallajökull volcano, Iceland (Pedersen and Sigmundsson, 2006; Sigmundsson et al., 2010). Volcanic deformation is a complex phenomenon that can occur to various extents and over varying time scales. Deformation may not necessarily be indicative of a pending eruption — for example, the Three Sisters volcanic centre (central Oregon, Cascade Range) displayed ~14 cm of uplift between 1995 and 2001 without subsequent eruption (Dzurisin et al., 2006) and eruptions may also occur without any displacement being detected, e.g. Shishaldin volcano, Alaska (Moran et al., 2006).

In this study we assess the potential of InSAR in terms of measuring displacement rates at Colombian volcanoes. A 550 km long segment of the Colombian Northern Volcanic Zone (NVZ) was surveyed, using L-band SAR data acquired between December 2006 and September 2009, by the Japanese Advanced Land Observing Satellite (ALOS) (JAXA, 2009). Results were classified into four categories: volcanoes exhibiting deformation, atmospheric signal, incoherence and no deformation. Where deformation was observed, we employ modelling techniques to determine the most likely source parameters and interpret complementary field data to verify our observations. We also discuss the advantages of L-band interferometry and the effects of atmospheric delay.

1.1. Introduction to Colombian volcanism

South America is one of the most active volcanic regions on Earth, with four distinct volcanically-active segments extending along the Andes, from Colombia in the north to Chile in the south, known as the

* Corresponding author. Tel.: +44 1865 272000; fax: +44 1865 272072.
E-mail address: michelle.parks@earth.ox.ac.uk (M.M. Parks).

0377-0273/$ – see front matter © 2011 Elsevier B.V. All rights reserved.
doi:10.1016/j.jvolgeores.2011.02.007

Northern, Central, Southern and Austral Volcanic Zones. The NVZ extends for 900 km through Ecuador and Colombia, and is associated with the subduction of the Nazca plate beneath South America at a rate of 58 mm/yr (Trenkamp et al., 2002).

A previous C-band survey was undertaken at Galeras volcano (Zebker et al., 2000), but only one interferogram could be generated because of a lack of available data. Furthermore, the data quality was too poor to be able to make any interpretation. A recent large-scale survey has also been undertaken covering the whole of Latin America. The results of this study showed no deformation at any of the Colombian volcanoes (Fournier et al., 2010). However, this survey was aimed at identifying larger deformation rates, over longer time periods and on a regional scale.

The Smithsonian Institution (GVPa, 1994-) catalogues 15 active volcanoes in Colombia, which are concentrated on the Cordillera Central, the Cordillera Occidental and the Cauca-Patia depression (Stern, 2004). Colombia is dominated by large andesitic–dacitic stratovolcanoes. These account for 13 of the 15 active volcanoes (Table 1). This study focuses on Galeras volcano in particular and so this system is introduced in more detail in the following section.

1.2. Geology of Galeras volcano

Galeras volcanic complex lies approximately 10 km west of the city of Pasto (population approx. 330 000) (Fig. 1). Galeras consists of a cone within a crescent shaped rim of a paleo-volcano (formed during a summit collapse event occurring between 12 and 5 ka ago (Calvache et al., 1997)). Eruptions have occurred at the summit crater, as well as at a series of vents distributed around the rim. It is one of the most active Colombian volcanoes — 6 major eruptions have occurred in the last 4500 years, producing pyroclastic flows and extensive tephra deposits. The volcano's most recent phase of activity commenced in 1988, following 40 years of quiescence (Williams et al., 1990). The renewed activity comprised the emplacement of a lava dome in late 1991, followed by a series of vulcanian eruptions from the summit crater between 1992 and 1993 (Stix et al., 1997). On 14 January 1993, an unexpected eruption at Galeras killed 6 volcanologists and 3 tourists during a field trip organised as part of the UN's Decade for Natural Disaster Reduction Workshop in Pasto (Baxter and Gresham, 1997). After 7 years of relative quiet, activity resumed in March 2000, culminating in 2 explosive eruptions from the El Pinta vent (east of the main crater) in 2002 and 2004, and additional eruptions from the summit crater in 2005, 2007, 2008, 2009 and 2010 (GVPb, 1994-). This study examines data covering the period of unrest between October 2007–January 2008 (including a VEI 1 eruption on 17 January 2008), dome growth during October 2008–February 2009 and a series of explosions occurring between February and June 2009. The volcano continues to display signs of activity at the time of writing. A comprehensive monitoring network has been established at Galeras, including broadband seismometers,

Table 1
Summary of Colombian volcanoes.

Name	Elevation (m)	Last eruption	VEI	Morphology	Eruptive characteristics
Romeral	3858	5950 BC +/−500 yrs	4?	Complex volcano.	Plinian eruptions.
Cerro Bravo	4000	1720 +/−150 yrs	4	Dacitic lava dome complex.	Dome extrusion and pyroclastic flows.
Nevado del Ruiz[a,b]	5321	Apr 1994–uncertain Sep 1985–Jul 1991	Unknown 3	Summit comprises a series of lava domes and two parasitic cones.	Phreatic eruptions, pyroclastic flows, surges and lahars.
Santa Isabel[c]	4965	2800 BC +/−100 yrs	Unknown	Elongated summit consists of a series of arc shaped domes.	Lava flows and pyroclastic flows.
Nevado del Tolima[c]	5220	Mar 1943	2	Consists of a series of lava domes and a funnel-shaped crater.	Dacitic lava flows, pyroclastic flows and lahars.
Cerro Machín[f,e]	2750	820 +/−100 yrs	3	2.4 km wide tuff ring crater comprising three lava domes.	Pyroclastic flows and lahars.
Nevado del Huila[c,d]	5364	Feb 2007–2010 (continuing)	3?	Elongated NS trending glacial-capped volcanic chain. Hot springs and fumaroles.	Phreatic eruptions, radial fissure eruptions, dome extrusion, ash falls and lahars.
Puracé	4650	Mar 1977	2	Truncated cone comprising of an inner 500 m wide crater containing fumaroles. Overlies dacitic shield volcano.	Pyroclastic flows, lahars and lava flows.
Sotará	4580	Unknown	Unknown	Site of active fumaroles and hot springs.	No historical eruptions known.
Volcán Petacas	4054	Unknown	Unknown	Lava dome.	No historical eruptions known.
Doña Juana	4160	Nov 1897–Aug 1936	4	Consists of two calderas and a series of lava domes.	Dome extrusion, lava flows, pyroclastic flows and lahars.
Galeras[g,h]	4276	Oct 2008–2010 (continuing)	1?	Consists of a cone within an older volcano — open to the west.	Pyroclastic flows, lahars, dome extrusion.
Azufral[i]	4070	930 BC?	4?	Crescent shaped acid lake, fumaroles and dacitic lava dome complex.	Lava flows, dome extrusion and pyroclastic flows.
Cumbal[j]	4764	Dec 1926	2	Lava dome within a 250 m wide crater. Hot springs and fumaroles.	Lava flows, pyroclastic flows and lahars.
Cerro Negro de Mayasquer	4470	Jul 1936?	2	Small crater lake within a caldera.	Lava flows.

Information was primarily compiled from the Smithsonian Institution, Global Volcanism Program (GVPa, 1994-) and Instituto Colombiano de Geologia y Mineria (INGEOMINAS, 2010a) websites.

[a] Additional reference: Williams, 1990a, 1990b.
[b] Additional reference: Banks et al., 1990.
[c] Additional reference: Huggel et al., 2007.
[d] Additional reference: Pulgarín et al., 2001.
[e] Additional reference: Thouret et al., 1995.
[f] Additional reference: Murcia et al., 2010.
[g] Additional reference: Calvache et al., 1997.
[h] Additional reference: Cortés and Raigosa, 1997.
[i] Additional reference: Bechon and Monsalve, 1991.
[j] Additional reference: Lewicki et al., 2000.

gas and infrasound sensors, electronic tiltmeters and a weather station (Seidl et al., 2003).

2. Methods and data quality

2.1. InSAR

Active satellites, such as ALOS, illuminate a swath of the earth's surface with electromagnetic radiation and record the backscattered waves. If the volcano deforms during the repeat period of the satellite (for ALOS this is 46 days), the displacement can be measured by observing the difference between the two radar returns when the satellite is in approximately the same position overhead. This path difference results in a phase shift, which can be detected by computing an interferogram (Massonnet and Feigl, 1995). The phase change observed in a single interferogram is the result of a combination of differences in orbital position, topography, atmospheric delay and ground deformation. To separate out the phase change resulting from deformation only, the other components must first be removed. Throughout this study, processing was undertaken using the Repeat Orbit Interferometry Package (ROI_PAC) (Rosen et al., 2004), the topographic correction was applied using the Shuttle Radar Topography Mission (SRTM) 90 m resolution digital elevation model (DEM) (Gesch et al., 2006) and interferograms were unwrapped using the branch cut algorithm (Goldstein et al., 1988).

InSAR has the ability to measure deformation over large areas (60×60 km) at high resolution (~90 m) with accuracies better than 1 cm. However, measurements of displacement rates at stratovolcanoes are notoriously difficult (Zebker et al., 2000; Pritchard and Simons, 2004). In order to successfully measure ground displacement, the ground surface needs to remain relatively unchanged between acquisitions, which is why the steep slopes and often snow covered peaks of stratovolcanoes produce areas of decorrelation. Highly vegetated areas, which are common in the tropics, can also be problematic. The coherence of ALOS L-band ($\lambda = 23.6$ cm) interferograms is typically higher than that obtained using C-band data ($\lambda = 5.65$ cm) from other satellites (e.g. RADARSAT or ENVISAT). This has now allowed measurements at volcanoes in tropical vegetated regions such as Arenal (Ebmeier et al., 2010) and Tungurahua (Biggs et al., 2010).

2.2. Atmospheric contributions

Changes in apparent path length can be caused by variations in temperature, pressure and water vapour in the troposphere, although path delays resulting from variations in water vapour are typically more common. Two types of tropospheric delay are prevalent in InSAR results. The first is caused by turbulent mixing in the atmosphere, which affects all landscapes (both rugged and flat terrain). The second type is caused by stratification and affects mountainous regions. Atmospheric delay from stratification is caused by variations in vertical refractivity profiles in either of the two SAR acquisitions (Hanssen, 2001). This type is of most concern with regards to the interpretation of volcanic deformation. Phase delays

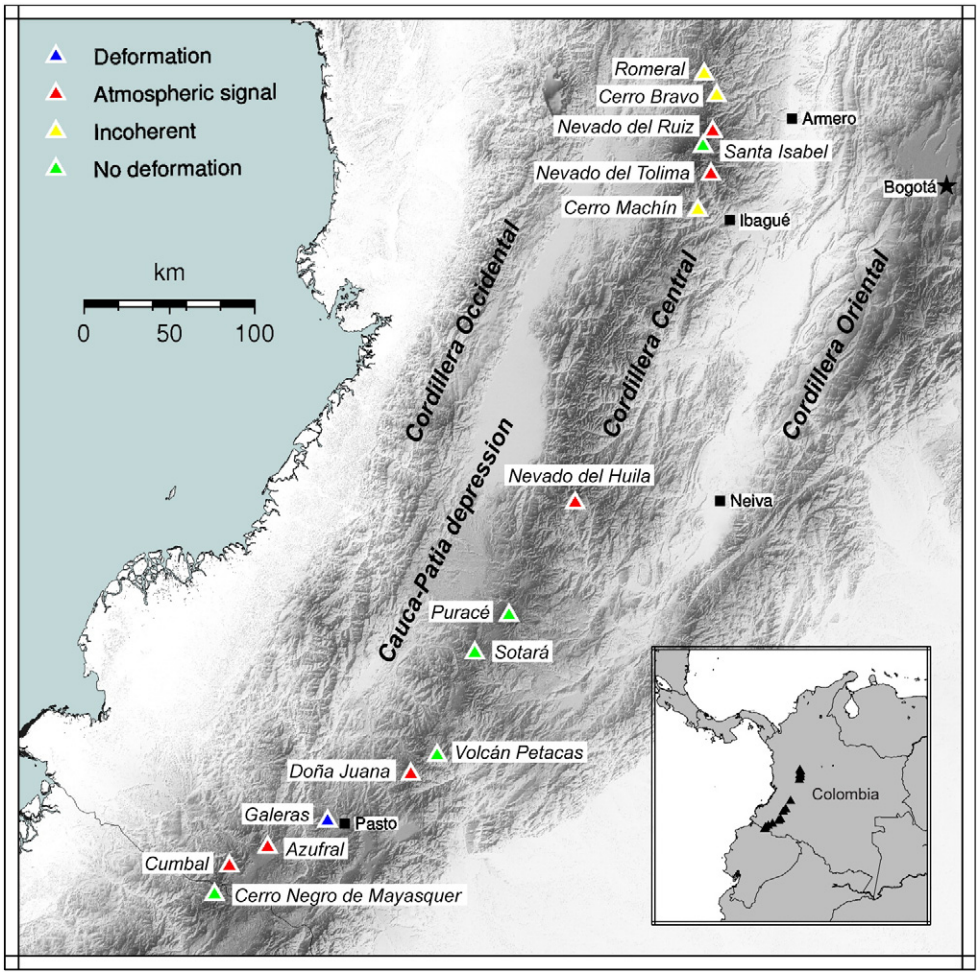

Fig. 1. Digital elevation model showing the location of Colombia's 15 active volcanoes (Table 1) and results of the InSAR study. The location of Bogotá is displayed as a black star and other major settlements as black squares. Inset shows location of the Colombian volcanic chain.

can be up to 11 cm (Heleno et al., 2010), which is well within the range of expected uplift or subsidence during volcanic unrest. The effects are generally observed over the highest peaks, which often correspond to volcanic edifices. Fortunately these effects have a strong correlation with topography, aiding their identification.

2.3. Data integrity

We employed stacking throughout the study in order to reduce random atmospheric noise. This technique consists of averaging a number of interferograms to enhance the signal to noise ratio. Interferograms displaying noise in the vicinity of the anomaly were not incorporated in the stack, to avoid bias in the averaged interferogram. Direct comparisons were then made between the DEM and the stacked interferogram, to assess the likely occurrence of phase variations related to stratified water vapour. The majority of interferograms used in the analysis have small perpendicular baselines ($B_\perp$), (Supplementary Table 1) which ensures that the altitude of ambiguity (difference in elevation responsible for producing a full fringe (12 cm) of deformation) is significantly larger than the error in the SRTM data. Comparisons were also made between $B_\perp$ and phase to identify any trends that may be indicative of an error in the DEM (e.g., Hooper et al., 2004).

Where appropriate, source modelling was undertaken using the University of Miami's GeodMod software (GeodMod, 2011) to establish the most likely source parameters to explain the observed deformation. Some of the methodology of GeodMod is described by Amelung and Bell, 2003. We used a simulated annealing inversion technique to determine the optimal source geometry and a linear inversion to compute the source strengths and simultaneously solve for a linear ramp to compensate for long-wavelength artefacts in the interferograms. Atmospheric noise is considered to be the largest contributor to error in the analysis. The magnitude of the water vapour contribution was estimated by fitting a 1D covariance function to each of the interferograms (Wright et al., 2003). Confidence intervals were estimated using a Monte Carlo type algorithm. We simulated 100 sets of atmospheric noise with the same magnitude and spatial correlation as the original interferograms. These were added to each of the input interferograms and the inversion was re-run to determine the range and trade-offs between each of the parameters (Wright et al., 1999; Biggs et al., 2009).

3. Results and discussion

One hundred interferograms (Supplementary Table 1) were analysed as part of this study to determine whether any of the Colombian volcanoes were exhibiting signs of deformation. Fig. 1 summarises the results of the analysis. Of the 15 volcanoes studied, 1 is believed to have undergone deformation during the observation period (Galeras), 6 are affected by atmospheric delay (Nevado del Ruiz, Nevado del Tolima, Nevado del Huila, Doña Juana, Azufral and Cumbal), 3 are incoherent (Romeral, Cerro Bravo and Cerro Machín) and the remaining 5 show no signs of deformation (Santa Isabel, Puracé, Sotará, Volcán Petacas and Cerro Negro de Mayasquer). Each of these categories will be discussed in more detail in the following section; however the main focus of the discussion is Galeras.

3.1. Galeras volcanic complex

Numerous studies have been undertaken at this volcano, with correlations made between variations in SO_2 emissions, tilt, the duration and amplitude of LP events and the onset of eruptions (e.g., Fischer et al., 1994, Ordóñez and Rey, 1997; Narváez et al., 1997). Volume changes associated with inflation or deflation of the magma chamber have also been derived by modelling variations in tilt (Ordóñez and Rey, 1997 and Narváez Medina, unpub. data). InSAR is a complementary technique which provides insight into patterns of magma movement and storage and may be used to optimise the placement of ground monitoring equipment.

3.1.1. InSAR

Eight interferograms generated between June 2007 and September 2008, from ALOS tracks 152 and 153, display an anomaly on the northeast-east flank of Galeras volcano that is equivalent to approximately 3 cm of vertical subsidence. Three interferograms are independent — that is, they do not share a common master or slave date (Fig. 2). This confirms that the anomaly cannot be the result of noise or atmospheric conditions on one particular date, and the interferograms span sufficiently different time periods for phase changes resulting from seasonal variations to be limited. The location of the peak deformation varies slightly in each of these interferograms due to differences in atmospheric conditions, variations in the viewing geometry of the satellite on different acquisition dates and the varying degrees of temporal coverage of each of the interferograms. Phase variations observed between interferograms covering different time periods may reflect subsurface processes such as post-eruptive relaxation of the magma chamber, magma recharge and degassing or surface processes related to ground instability or changes in atmospheric conditions.

A stack of seven interferograms from tracks 152 and 153 (Fig. 3A) clearly shows subsidence on the NE flank of the volcano. The maximum average displacement is −2.8 cm in the satellite's line of sight (LOS), which assuming purely vertical deformation corresponds to 3.4 cm of subsidence. Although one additional interferogram also displayed subsidence, this was affected by noise in the vicinity of the summit (Supplementary Table 1) and was not included in the stack. As the stack was generated by averaging interferograms from multiple tracks, it should be noted that the satellite's line of sight changes across the swath by ~10%, leading to an inherent error in the extracted deformation measurements (of order 10%). Comparing profiles of displacement with that of topography (Fig. 3B), we find that the phase increase is offset from the peak elevation, making it unlikely that the phase change is caused by stratified water vapour.

A subsidence signal may be caused by many processes, including co-eruptive deflation of a crustal magma reservoir, post-eruptive viscoelastic relaxation, edifice collapse, lava subsidence, degassing or depressurisation of a hydrothermal reservoir (e.g., Hurwitz et al., 2007). Only by refining the period of observed deformation, undertaking source modelling and comparing InSAR results with field observations, is it possible to differentiate between these various physical processes. Analysis of the interferogram time coverage plot (Fig. 4), suggests that the bulk of the deformation occurred during the 6 weeks between 4 December 2007 and 19 January 2008. This coincides with an explosive eruption at Galeras on 17 January 2008 (INGEOMINAS, 2008), during which incandescent blocks and bombs were ejected from the main crater and ash was dispersed up to 70 km to the west of the volcano. Preliminary analysis by INGEOMINAS scientists suggested that ~80% of the material ejected during the eruption was juvenile magma (INGEOMINAS, 2008).

3.1.2. Modelling

We tested both a point source (Mogi, 1958) and an Okada dislocation model (sill) (Okada, 1985) to determine the approximate source location, depth and volume change responsible for the observed deflation at Galeras. These are flat earth models that assume a pressure source in a homogeneous, isotropic, elastic half-space.

The best fitting model is the deflation of a rectangular dislocation, which can be thought of as a sill, situated at a depth of ~2 km and corresponding to a volume change of approximately -6.5×10^5 m^3 (Table 2; Fig. 5D and F). The sill is near-horizontal with an approximate length and width of 8 km and 3 km respectively. The dimensions, depth and dip of the sill considered suggest that the displacement resulted from the deflation of a thin magma lens, beneath the NE flank

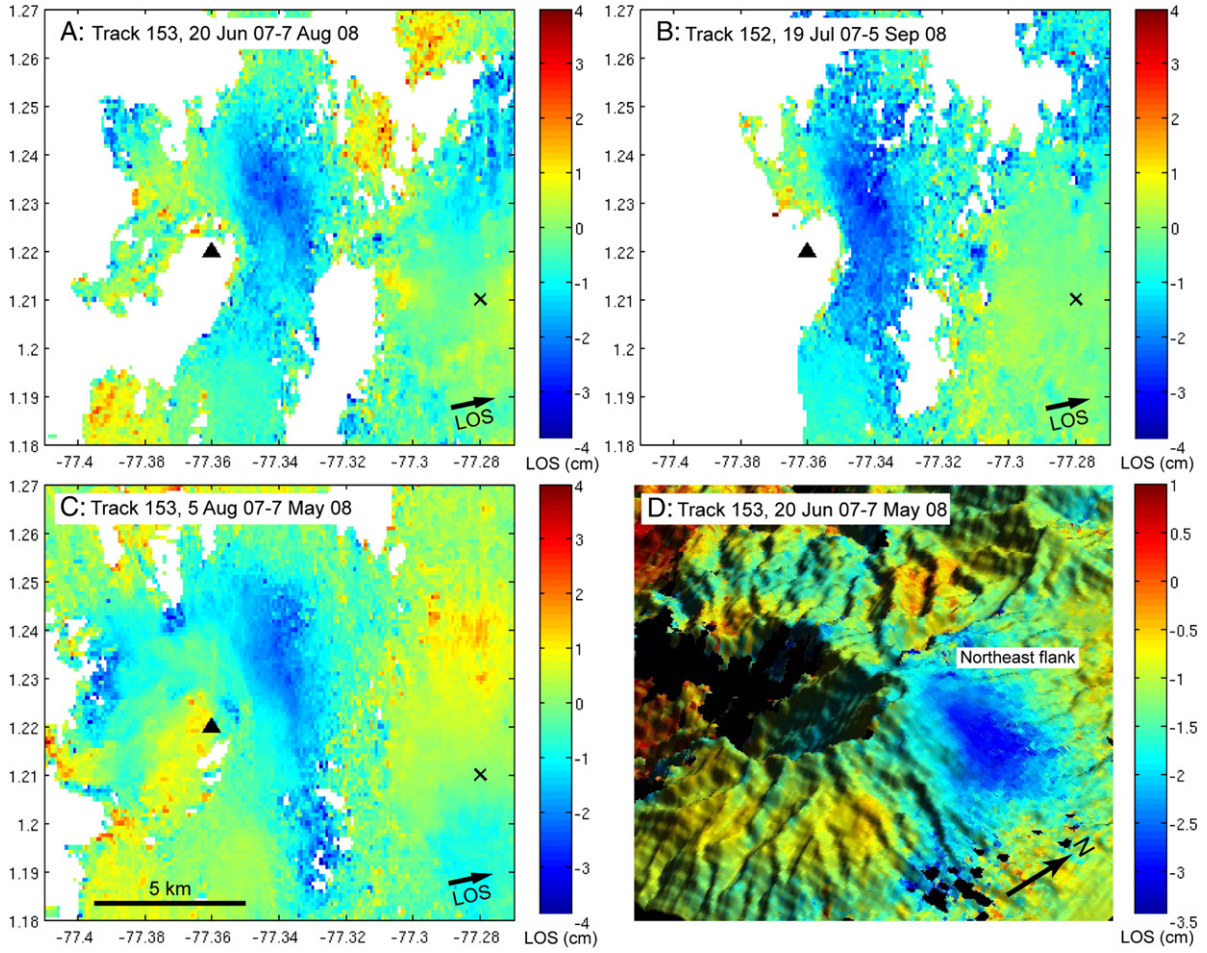

Fig. 2. L-band interferograms generated over Galeras for the period June 2007–September 2008. A) 20 Jun 07–07 Aug 08. B) 05 Aug 07–07 May 08. C) 19 Jul 07–05 Sep 08. D) Perspective view of interferogram 20 Jun 07–7 May 08 superimposed on a shaded relief DEM. The subsidence signal is displayed on the NE flank of the volcano, corresponding to ~−3 cm. The amplitudes of the independent interferograms A–C are given relative to a common reference point, displayed as a cross. The triangle marks the location of the summit at Galeras volcano.

of the volcano. Although the RMS misfit is comparable for both the Mogi point source and Okada sill, the Okada sill provides the best fit to the data, producing an elongated ellipsoidal pattern similar to the observed displacement (Fig. 5A and D).

The magnitude of the water vapour contribution was estimated by fitting a 1D covariance function to each of the interferograms (Wright et al., 2003). For a single interferogram the amplitude was ~6 mm. If the errors were uncorrelated, a stack of N observations with error (σ)

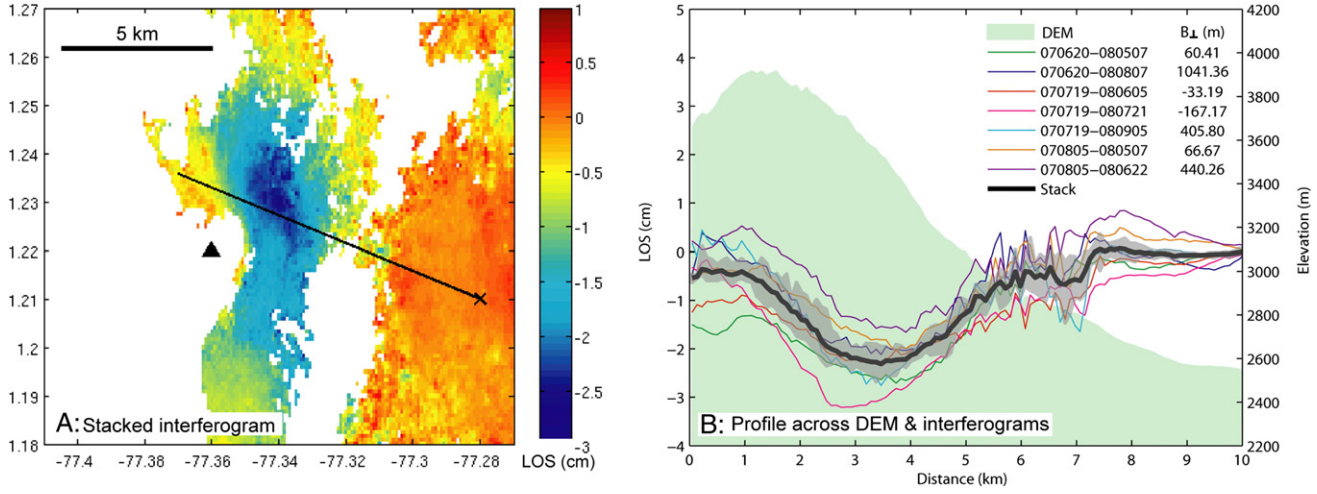

Fig. 3. A) Galeras stacked interferogram, derived by averaging 7 L-band interferograms from tracks 152 and 153 over the period 20 June 2007–5 September 2008. The reference point used to scale amplitudes is displayed as a cross and the traverse used for extracting phase and elevation data is shown as the NW-SE trending line. The triangle marks the location of the summit at Galeras volcano. B) Profiles extracted from interferograms and DEM across Galeras. Profiles across individual interferograms are displayed as thin coloured lines. The profile across the DEM is displayed as the green shaded area. The profile across the stacked interferogram is displayed as the black line and the difference between minimum and maximum values as the grey filled area. Interferogram master and slave dates are in the format yymmdd.

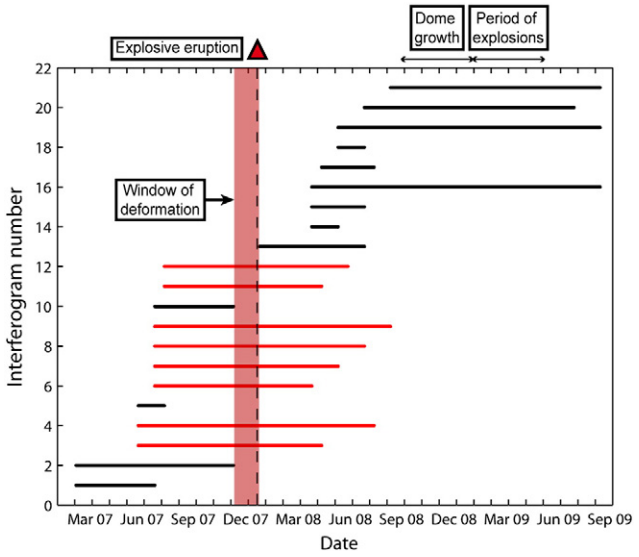

Fig. 4. ALOS interferograms used in the analysis at Galeras (from 3 March 2007 to 8 September 2009). Interferograms displaying subsidence at the volcano are displayed in red. Red shaded area represents time window during which the subsidence can have occurred. The red triangle and dashed line mark the explosive eruption at Galeras on 17 January 2008. Periods including dome growth and additional explosions are also annotated. Interferograms displaying significant atmospheric phase contributions are not included.

will have an error of $\sigma/\sqrt{N}$. Thus we expect the error on the averaged interferogram to be of the order 2 mm. This is in agreement with the observed RMS misfits between the forward models and the averaged interferogram (Table 2). We estimated the confidence intervals using a Monte Carlo type algorithm (Table 2). We simulated 100 sets of atmospheric noise which were added to each of the input interferograms and the inversion was re-run to determine the range and trade-offs between each of the parameters (Wright et al., 1999; Biggs et al., 2009). The primary trade-offs observed were between depth and the amount of opening, and depth and volume change (an increase in ΔV requires an increased depth to source to produce the same amount of displacement).

Although the point source (Mogi, 1958) and Okada dislocation (Okada, 1985) models do not take into account variations in topography, we tested a 1D model incorporating topographic corrections (Williams and Wadge, 1998) (Supplementary Fig. 1) for the profile displayed in Fig. 3B. Our results suggest only a minimal change would be observed, with a lateral displacement of the maximum amplitude to the east by approximately 500 m. Of course, a number of the assumptions made during modelling are unlikely to hold true. For example, the crust is unlikely to be homogeneous or isotropic in the vicinity of an active volcano and an intrusion of magma will heat the surrounding crust, producing weak thermally altered zones. By assuming a purely elastic, homogeneous half-space we possibly overestimate the depressurisation and underestimate the depth to the magma chamber (Masterlark et al., 2010). We also assume that the magma is incompressible; however it is likely to be a mixture of crystals, liquid and gas, and the behaviour of 3 phase liquids is poorly understood.

The derived volume change of -6.5×10^5 m^3 is close to the estimated erupted volume of 8.7×10^5 m^3, reported by INGEOMINAS (2008) for the 17 January eruption, which lends credibility to our interpretation of the deformation as resulting from deflation of the magma chamber during this small event. Although the modelling has inherent limitations, the modelled depth range, dimensions and location of the source are considered reasonable and are in broad agreement with contemporaneous tiltmeter data (INGEOMINAS, 2008 and Narváez Medina, unpub. data) discussed in Section 3.1.3, historic gravity anomalies (Jentzsch et al. 2004), a zone of low p-wave velocity (Londoño and Ospina, 2008), seismic attenuation anomalies (Carcolé et al., 2006; Lacruz et al., 2009) and cluster locations of historic seismic crises (Cortés and Raigosa, 1997) discussed further in Section 3.1.4. Previous petrological studies support magma storage at shallow levels beneath Galeras, with the majority of samples analysed from earlier eruptive phases showing evidence for amphibole instability (reaction rims replaced by oxides, pyroxene and plagioclaise). This suggests some magma residence at pressures of less than 2 kbar, assuming a temperature of 900 °C (Calvache and Williams, 1997).

The high spatial density of InSAR measurements has allowed us to identify a deformation source on the NE flank of Galeras. In light of this discovery, we review observations from sparser datasets (tilts and gravity) to see whether they are consistent with our InSAR measurements.

3.1.3. Observations from tiltmeters

We start by discussing other data, spanning the period of the 2008 activity covered by the InSAR signals. Two tiltmeters situated on the NE flank of the volcano registered displacement during the eruption on the 17 January 2008 — 'Crater', situated 0.8 km ENE, and 'Peladitos', located 1.4 km SE of the crater (Fig. 6A). Crater displayed variations in tangential and radial components of 24 and 26 microradians (μrads) respectively, while variations observed at Peladitos were 5 and 20 μrads (INGEOMINAS, 2008). Mogi modelling of the tilt data acquired between 17 and 19 January 2008 predicts a volume change of -7×10^5 m^3 with a deflation source located at a depth of 1.4 km (Narváez Medina, unpub. data). Both the volume and source depth computed from the tilt data correspond well with our InSAR modelling estimates of -6.5×10^5 m^3 and 1.8 km. Additional data are desirable to make a fully quantitative comparison of measurements. However, we can have confidence that the tilts are in agreement with the InSAR observations in that they also display subsidence, are in close proximity to the InSAR anomaly and are during the same window of deformation.

The detection of co-eruptive subsidence by two tiltmeters on 17 January 2008 and the fact that seismicity measurements recorded during January 2008 display a clear increase in LP events on 17 and 18 January (INGEOMINAS, 2008), lead us to believe that the displacement observed on the interferograms occurred on 17 January 2008. The occurrence of a VEI 1 eruption during the window of deformation suggests that the January 2008 subsidence signal was associated with co-eruptive processes within the magmatic and hydrothermal systems. Furthermore, the reasonable agreement between our model derived volumes and the estimated erupted volume suggests that the subsidence may be the result of magma withdrawal.

The January 2008 period was not the only occasion on which the tiltmeters have measured deformation at Galeras. Deformation believed to be associated with magma movement has been detected

Table 2
Source model parameters.

Source	RMS misfit (mm)	Depth (km)	Length (km)	Width (km)	Volume change (m^3)
Point source (Mogi)	3.06	2.8 ± 0.3	–	–	$-7.4\times10^5\pm1.9\times10^5$
Sill (Okada dislocation)	2.73	1.8 ± 0.2	7.9 ± 0.2	2.9 ± 0.2	$-6.5\times10^5\pm8.7\times10^4$

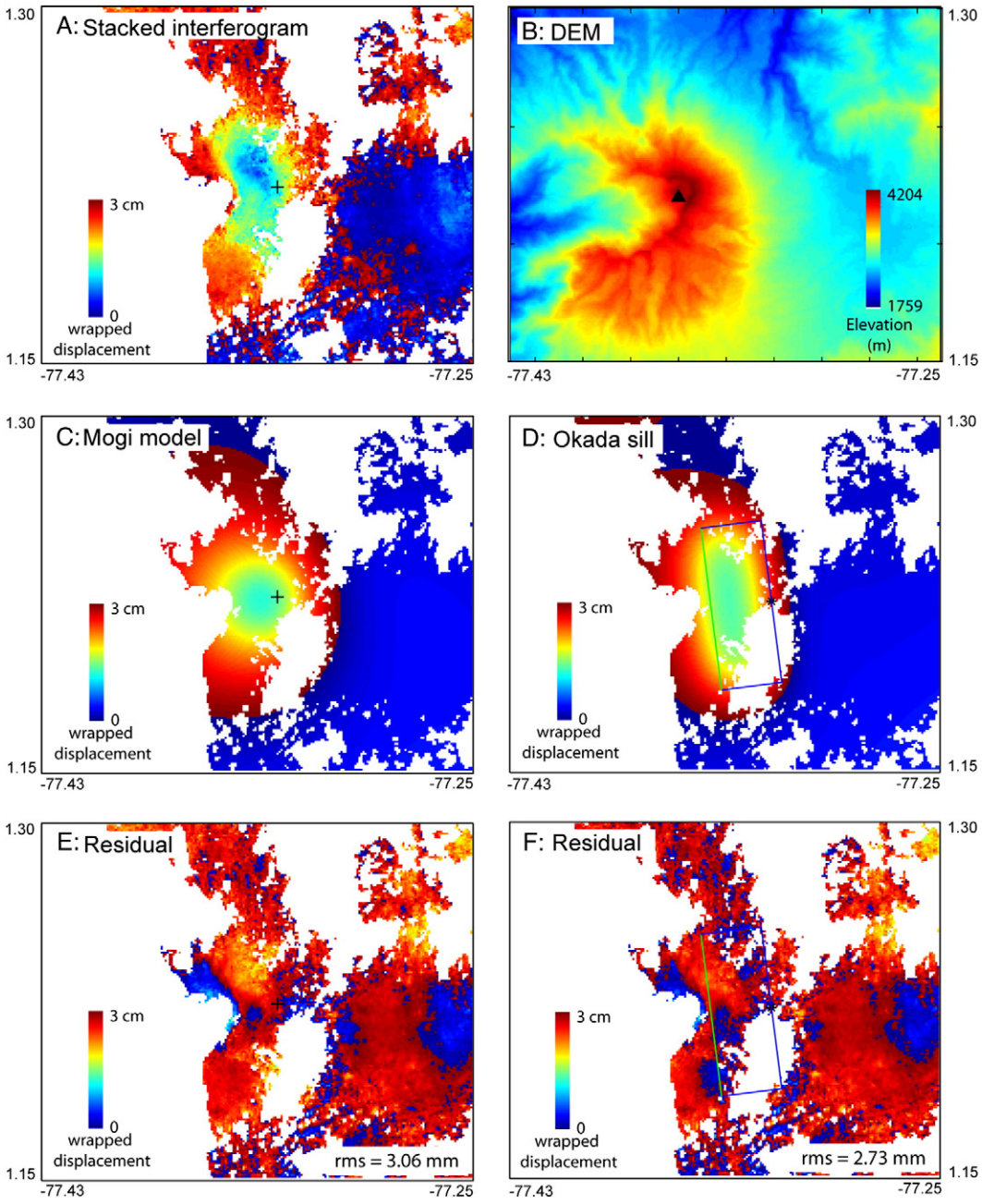

Fig. 5. Galeras 2D source modelling. A) Stacked interferogram. B) DEM. C) Modelled interferogram using Mogi point source. D) Best-fit model (Okada sill). E) Difference between stack and modelled interferogram in panel C. F) Difference between stack and modelled interferogram in panel D. The location of the Mogi point source is displayed as the cross in panels A, C and E. The outline of the Okada sill is displayed as the rectangle in panels D and F.

at both Peladitos and Crater on four other occasions: August–November 1991 (Ordóñez and Rey, 1997), August–October 2005, June–December 2008 and January–April 2009 (Narváez Medina, unpub. data). The first three periods were related to magma ascent and the extrusion of lava domes, whereas the decline observed during January–April 2009 is believed to be associated with a series of explosions occurring between 14 February and 29 April 2009 (Narváez Medina, unpub. data). The majority of interferograms spanning the periods June–December 2008 and January–April 2009, were either affected by stratified water vapour or showed long wavelength diagonal striping (caused by the dispersion of the radar wave by interactions with free electrons in the ionosphere (Gray et al., 2000; Hanssen, 2001)). After filtering attempts to reduce the atmospheric phase contribution, several interferograms displayed signs of possible deformation in accordance with the tilt measurements, but because remnant atmospheric phase variations still remained we did not undertake source modelling. Four interferograms covering both episodes (dome growth and explosions) display no deformation (Fig. 4). It is considered unlikely that dome growth alone would be detected via InSAR, as the length-scale is too short and interferograms span both of these periods, so this lack of observed deformation may be the result of any pre-eruptive deformation being cancelled by co-eruptive or post-eruptive deformation.

3.1.4. Evidence for a recurrent magma chamber

Our results are consistent with previous studies on Galeras since 1989. Although these earlier studies support the possibility of a recurrent chamber, InSAR provides the first piece of evidence linked to an eruption. Carcolé et al. (2006) suggested the presence of a shallow magma chamber beneath the NE flank of the volcano based on higher scattering coefficients of shallow earthquakes recorded

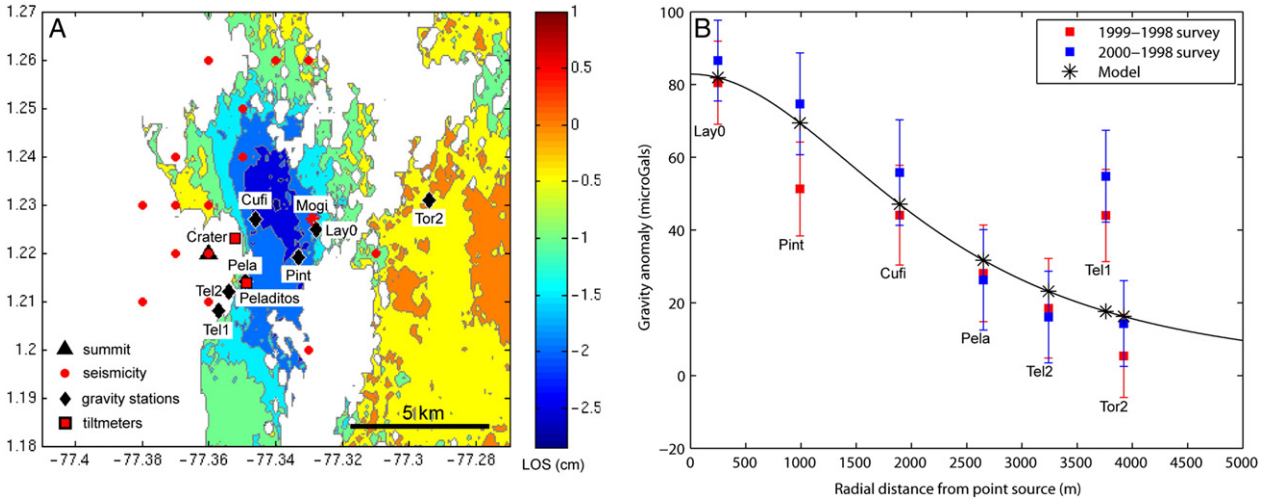

Fig. 6. Comparison of InSAR and field data at Galeras volcano. A) Stacked interferogram showing locations of seismic events recorded in Jan 2008, gravity stations and tiltmeters at Galeras volcano. B) Comparison of modelled gravity anomaly, $g_{z(t)}$ (assuming that the location and depth to the source are the same as for our 2008 InSAR measurements) and measured gravity data recorded at Galeras (after Jentzsch et al., 2004).

between 1989 and 2002, and Lacruz et al. (2009), utilising 435 VT events recorded during the same period, detected strong seismic attenuation anomalies to the NE of the crater (between latitudes 1.22 N to 1.28 N and longitudes −77.35 to −77.30 W) at depths between 2.5 and 5 km.

The position of our anomaly also corresponds with hypocentral cluster locations from 3 seismic crises in April 1993, November–December 1993 and March 1995 (Cortés and Raigosa, 1997). These events were located beneath the NE flank of the volcano at depths between 2 and 8 km below the surface. Stix et al. (1997) and Zapata et al. (1997) suggested that these events could be related to magma intrusion, whereas Jiménez et al. (2008) argued that these events may have resulted from the activation of local faults. In either case, it is feasible that previous tectonic earthquakes beneath the NE flank have resulted in zones of weakness providing preferential pathways for the migration of fluids. Furthermore, a tomographic inversion study undertaken by Londoño and Ospina (2008) identified a corresponding zone of reduced P-wave velocity. Their anomaly was located east of the crater at a depth of ~1–3 km beneath the summit, between longitudes −77.35 W and −77.32 W. The location is in good agreement with the position of our source of deflation derived from modelling. This low-velocity zone was interpreted by the authors as corresponding to a more fluid resident magma chamber.

Gravity campaigns undertaken by Jentzsch et al. (2004), between September 1998 and March 2000 detected an anomaly close to our observed subsidence signal (Fig. 6A shows the location of their gravity stations). The peak increases in gravity of 81 and 87 μGals (in the second and third campaigns respectively) were recorded approximately 3.5 km to the NE of the crater (Fig. 6B) (250 m from our modelled Mogi point source). The data indicates that the gravity increase occurred between acquisition of the first and second gravity surveys (over the 6-month period from September 1998–March 1999). The anomaly was observed in the same location one year later, when the third survey was undertaken.

Gravity measurements can be used to calculate changes in mass distribution, while deformation measurements are sensitive to volume change. Where both are available simultaneously, it is possible to calculate the density of the intrusion directly (Battaglia et al., 1999). In this case only gravity measurements from 1998 to 2000 were available, but by assuming that the location and depth to the source are the same as for our 2008 InSAR measurements (Section 3.1.2), the corresponding changes in mass during the period 1998–2000 may be estimated. If we are able to fit the 1998–2000 gravity data using our 2008 source location, this also suggests some decadal-scale stability in terms of the shallow internal structures within the volcano.

A spherical body was chosen for the modelling because of its straightforward comparison with Mogi point source models. The gravity anomaly produced by a buried sphere is a combination of two phenomena — a change in mass distribution at depth, plus a change in height as a result of the pressure change (Segall, 2010). We refer to these separate contributions as 'g_{mass}' (the gravity anomaly resulting from the redistribution of mass) and 'g_{def}' (that resulting from the induced deformation). The gravity change resulting from the combination of these ($\delta g_z(t)$) is equal to:

$$\delta g_{z(t)} = \delta g_{mass} + \delta g_{def} \quad (1)$$

and

$$\delta g_{mass} = \frac{G\Delta M d}{(x^2 + d^2)^{3/2}} \quad (2)$$

where ΔM is the change in mass, d is the depth from the centre of the chamber to the measurement point on the surface, x is the horizontal distance from the centre of the chamber to the reference point and G is the gravitational constant (6.67×10^{-11} m^3 kg^{-1} s^{-2}).

Since no deformation was observed at tiltmeter Peladitos (or indeed at Crater), but a gravity anomaly of 30 μGals was observed at gravity station Pela (2.7 km from Mogi source) (Fig. 6B) between September 1998 and March 2000, we assume that the majority of the anomaly is the result of changes in mass. Large variations in gravity have been observed at other volcanoes with little or no corresponding elevation changes, including Etna (Rymer et al., 1995), Merapi (Jentzsch et al., 2004) and Kilauea (Johnson et al., 2010). Furthermore, while no eruption was reported during the time span between the first and second gravity surveys, tornillos and harmonic tremor were recorded during October 1998–January 1999 (GVPc, 1994-). Tornillos are low frequency quasi-monochromatic seismic signals (Chouet, 1992) which have previously been associated with the resonance of fluids or gas moving along migration pathways. Harmonic tremor is often detected during periods of degassing (Gil Cruz and Chouet, 1997). Both processes suggest mass transfer within the system. There were also reports from INGEOMINAS scientists of cracks appearing at the summit and numerous fissures emitting gas (GVPc, 1994-).

We model the effects of mass redistribution by employing a linear inversion technique to minimise the misfit between the calculated and observed gravity measurements at each of the 7 stations. The

distance to each station was computed radially from our Mogi point source location (used rather than the Okada sill for simplicity). The optimal ΔM was determined to be 9.7×10^{10} kg, which will be discussed in greater detail later in this section. The model (Fig. 6B) provides a good match to the measured data, with the exception of the observed value at station Tel1. The half-width of the observed gravity anomaly and the subsidence anomaly from the stacked interferogram were also computed, to compare the wavelength of the gravity and InSAR measurements. The derived values are in good agreement (~2 km — Figs. 6B and 3B), which supports our modelled source location and depth (2.8 km) being characteristic of the system 10 years prior.

Two small eruptions occurred on 21 March and 5 April 2000, after the gravity surveys were acquired. The description of grey/white emissions (GVPc, 1994-) suggests that these events had a phreatic component. Acid gas variations at active fumaroles and thermal springs provide evidence of an active but immature hydrothermal system at Galeras (Alfaro and Zapata, 1997), and pre-eruptive decreases in HCl/CO_2 ratios also suggest selective absorption of volatiles by a shallow hydrothermal reservoir (Fischer et al., 1996). In light of these observations, we consider two possible scenarios that could be responsible for the increase in gravity by causing a sub-surface variation in mass with little or no resultant deformation: 1) magma intrusion, devesiculation and degassing (e.g., Eggers, 1983; Rymer, 1994 and Crider et al., 2008) and 2) groundwater recharge/migration (e.g., Jachens and Roberts, 1985). A similar effect could also be produced by magma intrusion into pre-existing open fractures (e.g., Johnson et al., 2010).

Applying the source location parameters calculated from InSAR has allowed us to estimate the mass increase associated with the gravity increase observed between 1998 and 2000 as 9.7×10^{10} kg. Therefore by assuming typical density changes associated with scenarios 1 and 2 we can assess the volume of new material introduced to the system (Table 3) using the relationship $V=\Delta M/\Delta\rho$. It is assumed that this volume change is accommodated within the edifice without causing deformation, either by migration through open pores and fractures or in the magmatic scenario, as a result of degassing. For example, the magma intrusion and degassing scenario requires that the loss of volatiles from a vesiculated magma (via degassing over a 6 month period) is balanced by the influx of melt (Table 2) such that the pressure remains approximately constant.

A gravity increase related to groundwater replenishment might be accomplished by either meteoric recharge, or the migration of groundwater to this area, as a result of induced pore-pressure gradients. Groundwater flow along open faults and fractures (Jónsson et al., 2003) might also explain the decline detected on two portable tiltmeters (Chorrillo and Huairatola) to the north of the volcano (between late September 1998 to the end of January 1999, the instruments showed a cumulative decline in the radial component, of ~35 and ~600 μrads at Chorrillo and Huairatola respectively (GVPc, 1994-)).

The meteoric recharge model requires a volume change of 5.4×10^8 m^3 (Table 3). Loboguerrero and Gilboa (1987) estimated the volume of the average groundwater recharge in the Cauca valley (NE of Galeras) to be ~1.6×10^5 m^3/yr/km^2. If we assume the recharge zone at Galeras comprises the region east of the amphitheatre margin, incorporating the active cone and fumaroles, this equates to an area ~0.8 km^2. Over the 6-month period (in which the gravity increase was observed) this would correspond to a volume of water accumulation of 6.3×10^4 m^3, which is too low to account for the gravity anomaly. Groundwater migration meanwhile would require a lateral fluid flux of 35 m^3 s^{-1} (Table 3) to produce the detected increase in gravity. This is significantly higher than that which has been reported in this area (~0.001 to ~0.3 m^3 s^{-1}, Loboguerrero and Gilboa, 1987; Fischer et al., 1997). Therefore meteoric recharge or lateral fluid flow alone does not seem sufficient to account for the observed anomaly.

Our preferred interpretation is that magmatic processes are a more probable explanation of the gravity anomaly. The model yields injection rates (~6 m^3 s^{-1}) comparable to those seen at other andesitic volcanoes such as Soufrière Hills, Montserrat (Elsworth et al., 2008; Melnik and Sparks, 2005). Although the gravity anomaly cannot be explained solely by groundwater recharge/migration, we do not discount the interaction between magma intrusion and degassing, and the selective absorption of soluble volatiles into shallow ground waters, during sealing of migration pathways, which may have led to the repeated episodes of pressure build-up and eruption (e.g., Fischer et al., 1996; Boichu et al., 2008).

In summary, from a combination of independent observations (InSAR and tilts), source modelling and the episodic nature of the observed displacement, we infer that the 2008 subsidence measured at Galeras is likely to have resulted from processes related to the explosive eruption occurring in January 2008. It is proposed that during this event the expulsion of gas and ash caused a reduction in pressure of a magma chamber, situated ~2–3 km NE of the summit at a depth of ~2 km. This new understanding of the shallow volcanic system at Galeras in 2008 has allowed us to re-examine the nature of the activity and the gravity anomaly observed between 1998 and 2000. We are able to model this data successfully using the same source parameters as for 2008, suggesting some stability in the subsurface structure on a decadal timescale. Based on volumetric calculations and visual observations it would seem that the small eruptions in 2000 were most likely a combination of both hydrothermal and magmatic processes.

3.2. InSAR survey of Colombian volcanoes

Although the volcanoes discussed in this section are not thought to be deforming, we have included a brief review of our results. Many of these volcanoes are of great interest to the scientific community and to others concerned with hazard management.

3.2.1. Atmospheric signals

Interferograms covering Nevado del Ruiz, Nevado del Tolima, Nevado del Huila, Doña Juana, Azufral and Cumbal appear to be affected by tropospheric delay. These displayed significant phase changes during the observation period, but in each case displacement could either be correlated with topography or was reversible with seasons. At Nevado del Tolima, a possible subsidence signal (increase

Table 3
Parameters used to model 2 possible scenarios that may be responsible for the observed increase in gravity at Galeras.

Model	ρ_2 (kg m^{-3})	ρ_1 (kg m^{-3})	$\Delta\rho$ (kg m^{-3})	V (m^3)	Minimum inferred rate of fluid movement[a] (m^3 s^{-1})
Magma intrusion, devesiculation and degassing[b]	2600	1600	1000	9.7×10^7	6
Groundwater recharge/migration[c]	1000	0	180	5.4×10^8	35

[a] Computed by assuming fluid movement was evenly distributed over the 6-month period between the 1998 and 1999 gravity campaigns. Magma densities were computed using KWare Magma (KWare, 1999) assuming an andesitic magma, at a temperature of 900 °C and pressure of 900 bars (corresponding to ~3 km depth). ρ_1 is the density of the material in place, ρ_2 is the density of the intruding material, $\Delta\rho$ is the overall change in density and V is the volume of new material introduced to the system, associated with the change in mass (it is assumed that this volume change is accommodated within the edifice without causing deformation, either as a result of degassing or intrusion into open pores and fractures).
[b] Modelled by replacing a vesiculated magma (1600 kg m^{-3}) with an unvesiculated magma.
[c] Assuming an average porosity of 18% and meteoric water with a density of 1000 kg m^{-3} is filling empty voids resulting in an overall increase in density of 180 kg m^{-3}.

in range) was observed on multiple interferograms from separate tracks (Fig. 7A and B). However each of these spanned the latter half of the calendar year and a decrease in range was detected on an interferogram covering 12 August 2007–29 June 2008. The apparent reversal in polarity and comparison of displacement and DEM (Fig. 7B) suggests that this is likely the result of seasonal variations in water vapour.

Doña Juana is potentially one of the most hazardous volcanoes in Colombia, due to its history of large eruptions (>VEI 4) and capacity for generating major pyroclastic flows. At Doña Juana several interferograms exhibit phase changes of up to 4 cm of displacement in the satellite's LOS. However, a NE-SW traverse across the anomaly from the interferogram 19 July 2007–3 September 2007 shows that the extracted phase is highly correlated with topography (Fig. 7D). Doña Juana and Cerro Animas (peak to the NE) have roughly the same relief (~4150 m) and similar phase change. This would seem to be a clear example of the effect of stratified water vapour. There is some recent evidence for new activity in the region of Doña Juana and Cerro Animas. VT earthquakes were recorded on 20 and 21 May 2009, (INGEOMINAS, 2009) and a cluster of earthquakes were detected in June 2010, in close proximity to Cerro Animas (Monsalve, unpub. data). The 2 interferograms covering the first period of seismic activity (May 2009) are affected by tropospheric delay so additional scenes will be required to determine whether this volcano is deforming.

After 450 years of quiescence, activity resumed at Nevado del Huila in February 2007, with a VEI 3 explosive eruption that produced damaging mudflows. Successive eruptions followed in November 2008 and October 2009 (GVPd, 1994-). Nevado del Huila displayed possible uplift on one interferogram covering the period 17 March 2008 – 18 December 2008 (Supplementary Fig. 2). Although the observed anomaly coincides with the most recent periods of activity (2 January 2008 - April 2008 and 26 October 2008–2010 (GVPe, 1994-)), the phase signature over the summit appears correlated with topography. This suggests phase variations are the result of stratified water vapour. There is however an anomaly on the western flank (~3.5 cm) that is offset from the DEM (Supplementary Fig. 2), but this was only visible on one interferogram and so cannot be viewed as conclusive.

Nevado del Ruiz has a propensity for creating large destructive lahars. The November 1985 eruption produced small pyroclastic flows and surges that melted part of the ice-cap. This generated lahars that crashed through the towns of Armero and Chinchina (Naranjo et al., 1986). Nevado del Ruiz displays a decrease in range (~2.5 cm LOS) on one interferogram. This was not observed at any of the 3 other volcanoes, which were also covered by the image 11 December 2007–13 December 2008 (Supplementary Fig. 3). Using additional interferograms which show no deformation, we narrow down the time window to between 27 April 2008 and 28 July 2008. We attribute this anomaly to atmospheric contributions because no volcanic activity was reported for this time interval, the signal has a high correlation with topography and it was only observed for this one time period with no other supporting observations.

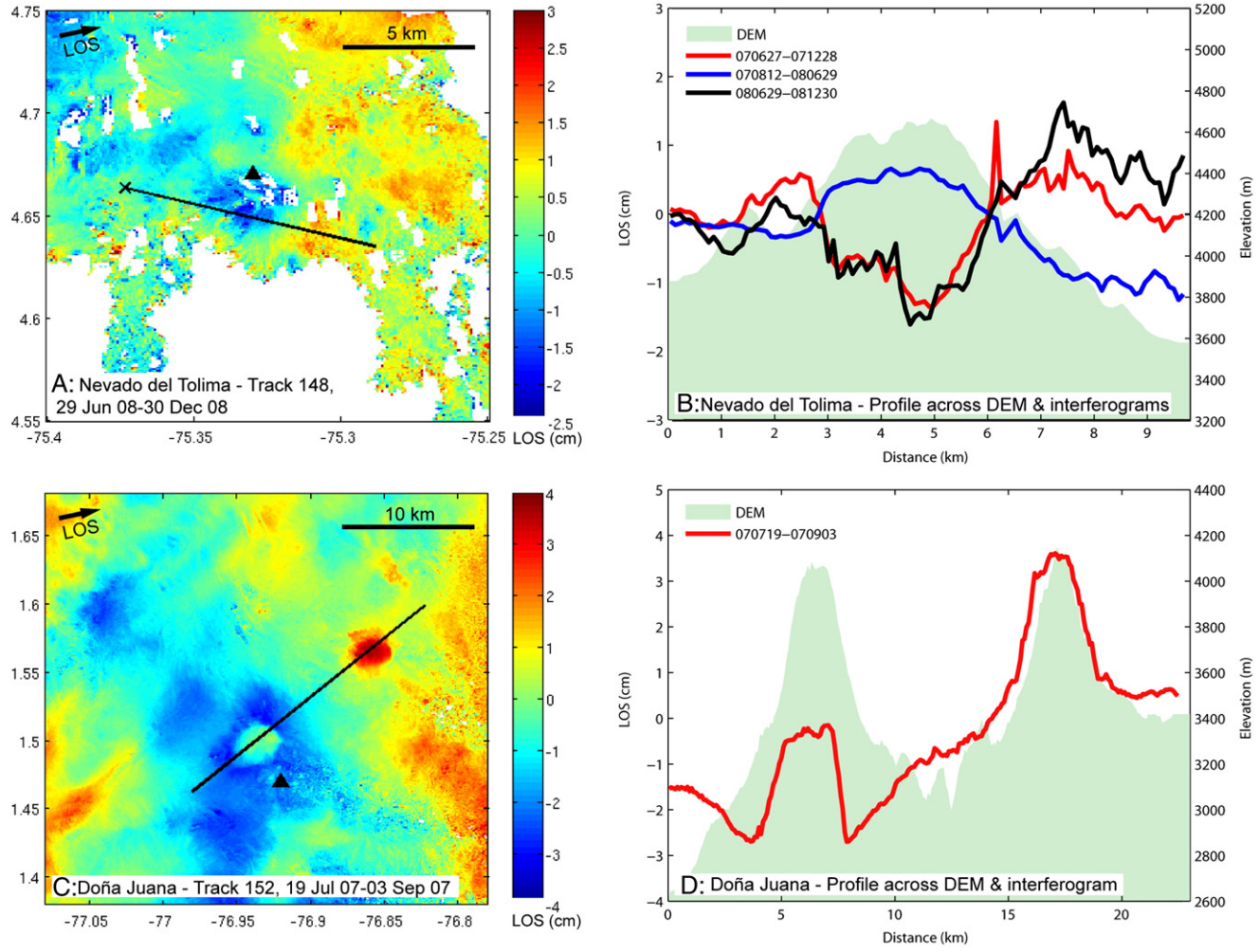

Fig. 7. A) Interferogram generated over Nevado del Tolima for the period 29 Jun 08–30 Dec 08. B) Profile extracted across DEM and interferograms for Nevado del Tolima. C) Interferogram generated over Doña Juana for the period 19 Jul 07–03 Sep 07. D) Profile extracted across DEM and interferogram for Doña Juana (SW) and Cerro Animas (NE). Interferogram master and slave dates in B and D are in the format yymmdd.

A number of interferograms from multiple tracks displayed long wavelength diagonal striping, possibly the result of ionospheric interactions (Gray et al., 2000; Hanssen, 2001). Although this kind of delay is unlikely to be misinterpreted as volcanic deformation, it may mask small displacement signals.

3.2.2. Volcanoes not displaying signs of deformation

No deformation was observed at Romeral, Cerro Bravo, Santa Isabel, Cerro Machín, Puracé, Sotará, Volcán Petacas and Cerro Negro de Mayasquer. It should however be noted that for several of these, InSAR coverage is limited by poor coherence (Romeral, Cerro Bravo and Cerro Machín). Cerro Machín (currently limited by coherence) is important to target because after four years of relative quiet, anomalous seismic activity was detected in the vicinity of the main dome in January 2008. This was followed by a seismic crisis on 9 November 2008 and swarms of shallow earthquakes on 18 December 2008 and 6 June 2009 (INGEOMINAS, 2010b). Unfortunately no interferograms covering these periods maintain coherence in the vicinity of the volcano. At the time of writing, the frequency of swarms at Cerro Machín appears to be increasing, with additional events occurring in December 2009, March 2010, July 2010 and September 2010.

4. Conclusions

Following the analysis of 100 interferograms, covering a 550 km segment of the Colombian NVZ between 2006 and 2009, we conclude that the majority of volcanoes are not exhibiting deformation. Of the 15 volcanoes surveyed, atmospheric signals have been observed at 6 (Nevado del Ruiz, Nevado del Tolima, Nevado del Huila, Doña Juana, Azufral and Cumbal), 5 displayed no sign of deformation (Santa Isabel, Puracé, Sotará, Volcán Petacas and Cerro Negro de Mayasquer), 3 were incoherent (Romeral, Cerro Bravo and Cerro Machín) and a subsidence signal was detected at 1 (Galeras).

Three independent interferograms over Galeras from two ALOS tracks display similar displacements, coinciding with the October 2007–January 2008 unrest and eruption. The maximum observed change corresponds to approximately −3 cm vertical displacement. We propose that this signal was caused by deflation of the magma chamber during an explosive event on 17 January 2008. Source models provide a good fit to the data and insight into the withdrawal volume, depth to source, and the dimensions of the chamber. The observed displacement is consistent with deflation of a magma lens under the NE flank of the volcano, caused by a volume change of -6.5×10^5 m^3 from a deformation source situated at a depth of ~2 km below the surface. This information may be useful in characterising part of the magma plumbing system. Prior studies, including gravity measurements (Jentzsch et al., 2004), deformation measurements (Narváez Medina, unpub. data), seismic attenuation studies (Carcolé et al. 2006; Lacruz et al. 2009) and a tomographic inversion (Londoño and Ospina 2008) all support the existence of a resident/recurring chamber at this location over a decadal timescale. This suggests that future field monitoring efforts could benefit by increasing deployment of equipment in this region.

Nevado del Huila also entered an eruptive phase during the observation period. However we were not able to confirm any deformation at this volcano. More frequent SAR acquisitions are required to better determine the deformation characteristics of this volcano. Atmospheric delay is the primary contributor to noise in interferograms. Atmospheric signals were identified at 6 volcanoes with Doña Juana and Nevado del Tolima providing good examples of phase variations resulting from a stratified troposphere. Santa Isabel, Puracé, Volcán Sotara, Volcán Petacas and Cerro Negro de Mayasque showed no signs of deformation, and no activity was reported at these volcanoes during the observation period. Coherence was limited at Cerro Machín, Cerro Bravo and Romeral. Cerro Machín has showed recent signs of seismic unrest and would benefit from additional observation.

This study highlights the potential use of InSAR for measuring displacement at active volcanoes, and demonstrates how combining the results with modelling and complimentary field data (e.g. gravity and tilts) can provide further confidence concerning the likely origin and dimensions of the source of deformation. We demonstrate that L-band interferometery provides improved coherence over C-band data at Galeras, but coverage is still limited by incoherence as well as by atmospheric delay at several volcanoes. Lack of observed deformation may be a result of limited SAR acquisitions or internal processes which offset surface displacements. This question may only be answered with increased coverage.

With the launch of new satellites such as Sentinel-1 and DESDynI (Deformation, Ecosystem Structure and Dynamics of Ice — a dedicated InSAR and LIDAR mission) acquisition parameters will be improved and satellite repeat times reduced (e.g. from 46 to ~12 days). More frequent observations would facilitate detection of renewed activity, while weekly/daily measurements during volcanic crises would provide a better understanding of both the magmatic processes involved and the potential hazard.

Supplementary materials related to this article can be found online at doi:10.1016/j.jvolgeores.2011.02.007.

Acknowledgements

The authors would like to thank Tim Wright, Sebastian Watt, Tony Watts, Chris Kilburn, Judith Woo, Jo Gottsmann and Antonio Costa for useful discussions. We thank Patricia Ponce (INGEOMINAS, Pasto) for her helpful correspondence; Diego Gómez (INGEOMINAS, Pasto) for providing seismicity data for the 2008 eruption at Galeras; Adelheid Weise (Institute of Earth Sciences, Jena) for providing data from their 1998–2000 gravity campaigns and Susanna Ebmeier for sharing her scripts, which were modified to generate Figs. 1 and 4. The manuscript was much improved by helpful reviews from Seth Moran and Tobias Fischer. All ALOS data were acquired from the Japan Aerospace Exploration Agency (JAXA) via the Alaska Satellite Facility (ASF). ALOS imagery: © JAXA, METI. MMP is supported by an NCEO studentship and JB is an ESA Changing Earth Science Network Fellow. MMP, JB, TAM and DMP are supported by and contribute to the NERC NCEO Dynamic Earth and Geohazards group.

References

Alfaro, C.M., Zapata, J.A., 1997. Acid gas emissions from Galeras volcano, Colombia, 1989–1994. J. Volcanol. Geoth. Res. 77, 209–228.
Amelung, F., Bell, J.W., 2003. Interferometric synthetic aperture radar observations of the 1994 Double Spring Flat, Nevada, earthquake (M5.9): main shock accompanied by triggered slip on a conjugate fault. J. Geophys. Res. 108, 2433. doi:10.1029/2002JB001953.
Banks, N.G., Carvajal, C., Mora, H., Tryggvason, E., 1990. Deformation monitoring at Nevado del Ruiz, Colombia-October 1985–March 1988. J. Volcanol. Geoth. Res. 41, 269–295. doi:10.1016/0377-0273(90)90092-T.
Battaglia, M., Roberts, C., Segall, P., 1999. Magma intrusion beneath Long Valley Caldera confirmed by temporal changes in gravity. Science 285, 2119–2122.
Baxter, P.J., Gresham, A., 1997. Deaths and injuries in the eruption of Galeras Volcano, Colombia, 14 January 1993. J. Volcanol. Geoth. Res. 77, 325–338.
Bechon, F., Monsalve, M.L., 1991. Activité récente préhistorique du volcan Azufral (S-W de la Colombie). C. R. Acad. Sci. Paris 313 (2), 99–104.
Biggs, J., Anthony, E.Y., Ebinger, C.J., 2009. Multiple inflation and deflation events at Kenyan volcanoes, East African rift. Geology 37 (11), 979–982.
Biggs, J., Mothes, P., Ruiz, M., Amelung, F., Dixon, T.H., Baker, S., Hong, S.-H., 2010. Stratovolcano growth by co-eruptive intrusion: the 2008 eruption of Tungurahua Ecuador. Geophys. Res. Lett. 37, L21302. doi:10.1029/2010GL044942.
Boichu, M., Villemant, B., Boudon, G., 2008. A model for episodic degassing of an andesitic magma intrusion. J. Geophys. Res. 113, B07202.
Calvache, V.M.L., Williams, S.N., 1997. Geochemistry and petrology of the Galeras Volcanic Complex, Colombia. J. Volcanol. Geoth. Res. 77, 21–38.
Calvache, V.M.L., Cortés, J.G.P., Williams, S.N., 1997. Stratigraphy and chronology of the Galeras volcanic complex, Colombia. J. Volcanol. Geoth. Res. 77, 5–19.
Carcolé, E., Ugalde, A., Vargas, C.A., 2006. Three-dimensional spatial distribution of scatterers in Galeras volcano, Colombia. Geophys. Res. Lett. 33, L08307. doi:10.1029/2006GL025751.
Chouet, B., 1992. A Seismic Model for the Source of Long-Period Events and Harmonic Tremor. In: Gasparini, P., Scarpa, R., Aki, K. (Eds.), Volcanic Seismology. : IAVCEI Proc. in Volcanol., 3. Springer-Verlag, New York, pp. 133–156.

Cortés, J.G.P., Raigosa, A.J., 1997. A synthesis of the recent activity of Galeras volcano, Colombia: seven years of continuous surveillance, 1989–1995. J. Volcanol. Geoth. Res. 77, 101–114.
Crider, J.G., Hill Johnsen, K., Williams-Jones, G., 2008. Thirty-year gravity change at Mount Baker Volcano, Washington, USA: extracting the signal from under the ice. Geophys. Res. Lett. 35, L20304. doi:10.1029/2008GL034921.
Dzurisin, D., Lisowski, M., Wicks, C.W., Poland, M.P., Endo, E.T., 2006. Geodetic observations and modeling of magmatic inflation at the Three Sisters volcanic center, central Oregon Cascade Range, USA. J. Volcanol. Geoth. Res. 150, 35–54.
Ebmeier, S.K., Biggs, J., Mather, T.A., Wadge, G., Amelung, F., 2010. Steady downslope movement on the western flank of Arenal volcano, Costa Rica. Geochem. Geophys. Geosyst. 11, Q12004. doi:10.1029/2010GC003263.
Eggers, A.A., 1983. Temporal gravity and elevation changes at Pacaya Volcano, Guatemala. J. Volcanol. Geoth. Res. 19, 223–0237.
Elsworth, D., Mattioli, G., Taron, J., Voight, B., Herd, R., 2008. Implications of magma transfer between multiple reservoirs on eruption cycling. Science 322, 246–248. doi:10.1126/science.1161297.
Fischer, T.P., Morrissey, M.M., Calvache, M.L., Gómez, D., Torres, R., Stix, J., Williams, S.N., 1994. Correlations between SO_2 flux and long-period seismicity at Galeras volcano. Nature 368, 135–137.
Fischer, T.P., Arehart, G.B., Sturchio, N.C., Williams, S.N., 1996. The relationship between fumarole gas composition and eruptive activity at Galeras Volcano, Colombia. Geology 24, 531–534.
Fischer, T.P., Sturchio, N.C., Stix, J., Arehart, G.B., Counce, D., Williams, S.N., 1997. The Chemical and Isotopic Composition of Fumarolic Gases and Spring Discharges from Galeras Volcano. J. Volcanol. Geoth. Res. 77, 229–253.
Fournier, T.J., Pritchard, M.E., Riddick, S.N., 2010. Duration, magnitude, and frequency of subaerial volcano deformation events: new results from Latin America using InSAR and a global synthesis. Geochem. Geophys. Geosyst. 11, Q01003. doi:10.1029/2009GC002558.
GeodMod, 2011. GeodMod [online]. Available: http://www.rsmas.miami.edu/personal/famelung/geodmod/geodmod.html. Last accessed 27 March 2011.
Gesch, D., Muller, J.P., Farr, T.G., 2006. The shuttle radar topography mission — data validation and applications, foreword to special issue. Photogramm. Eng. Remote Sens. 72, 233–235.
Gil Cruz, F., Chouet, B.A., 1997. Long-period events, the most characteristic seismicity accompanying the emplacement and extrusion of a lava dome in Galeras Volcano, Colombia, in 1991. J. Volcanol. Geoth. Res. 77, 121–158.
Goldstein, R.M., Zebker, H.A., Werner, C.L., 1988. Satellite radar interferometry: two-dimensional phase unwrapping. Radio Sci. 23, 713–720.
Gray, A.L., Mattar, K.E., Sofko, G., 2000. Influence of ionospheric electron density fluctuations on satellite radar interferometry. Geophys. Res. Lett. 27, 1451–1454.
GVPa - Smithsonian Institution, Global Volcanism Program (1994-). Volcanoes of South America (Colombia) [online]. Available: http://www.volcano.si.edu/world/region.cfm?rnum=1501. Last accessed 1 February 2011.
GVPb - Smithsonian Institution, Global Volcanism Program (1994-). Galeras [online]. Available: http://www.volcano.si.edu/world/volcano.cfm?vnum=1501-08=&volpage=erupt. Last accessed 1 February 2011.
GVPc - Smithsonian Institution, Global Volcanism Program (1994-). Galeras (Index of monthly reports) [online]. Available: http://www.volcano.si.edu/world/volcano.cfm?vnum=1501-08=&volpage=var#bgvn_2412. Last accessed 1 February 2011.
GVPd - Smithsonian Institution, Global Volcanism Program (1994-). Nevado del Huila [online]. Available: http://www.volcano.si.edu/world/volcano.cfm?vnum=1501-05=&volpage=weekly#Jul2010. Last accessed 1 February 2011.
GVPe - Smithsonian Institution, Global Volcanism Program (1994-). Nevado del Huila [online]. Available: http://www.volcano.si.edu/world/volcano.cfm?vnum=1501-05=&volpage=erupt. Last accessed 1 February 2011.
Hanssen, R.F., 2001. Radar Interferometry: Data Interpretation and Error Analysis. Kluwer Academic Publishers, pp. 130–159.
Heleno, S.I.N., Frischknecht, C., d'Oreye, N., Lima, J.N.P., Faria, B., Wall, R., Kervyn, F., 2010. Seasonal tropospheric influence on SAR interferograms near the ITCZ — the case of Fogo Volcano and Mount Cameroon. J. Afr. Earth Sci. doi:10.1016/j.jafrearsci.2009.07.013.
Hooper, A., Zebker, H., Segall, P., Kampes, B., 2004. A new method for measuring deformation on volcanoes and other natural terrains using InSAR persistent scatterers. Geophys. Res. Lett. 31, L23611. doi:10.1029/2004GL021737.
Huggel, C., Ceballos, J.L., Ramírez, J., Pulgarín, B., Thouret, J.C., 2007. Review and reassessment of hazards owing to volcano–ice interactions in Colombia. Ann. Glaciol. 45, 128–136.
Hurwitz, S., Christiansen, L.B., Hsieh, P.A., 2007. Hydrothermal fluid flow and deformation in large calderas: inferences from numerical simulations. J. Geophys. Res. 112, B02206.
INGEOMINAS, 2008. Instituto Colombiano de Geologia y Mineria — observatorio vulcanologico y sismologico de Pasto [online]. Available: http://intranet.INGEOMINAS.gov.co/pasto/images/a/a2/Resumen_actividad_Galeras_ene_14_2008_ene_20_2008.pdf. Last accessed 1 February 2011.
INGEOMINAS, 2009. Subdireccion de amenazas geologicas y entorno ambiental. Observatorio vulcanológico y sismológico de Pasto [online]. Available: http://intranet.ingeominas.gov.co/pasto/images/d/da/Informe_visita_may_2009_volcan_Dona_Juana.pdf. Last accessed 1 February 2011.
INGEOMINAS, 2010a. Principales volcanes de Colombia [online]. Available: http://intranet.ingeominas.gov.co/pasto/Principales_volcanes_de_Colombia. Last accessed 1 February 2011.
INGEOMINAS, 2010b. Instituto Colombiano de Geologia y Mineria - Informes_Tecnicos_del_Complejo_Volcanico [online]. Available: http://intranet.INGEOMINAS.gov.co/manizales/Informes_Tecnicos_del_Complejo_Volcanico. Last accessed 1 February 2011.
Jachens, R.C., Roberts, C.W., 1985. Temporal and areal gravity investigations at Long Valley Caldera, California. J. Geophys. Res. 90(11) 210–211, 218.
JAXA EORC, 2009. About ALOS — overview and objectives [online]. Available: http://www.eorc.jaxa.jp/ALOS/en/about/about_index.htm. Last accessed 1 February 2011.
Jentzsch, G., Weise, A., Rey, C., Gerstenecker, C., 2004. Gravity changes and internal processes: some results obtained from observations at three volcanoes. J. Appl. Geophys. 161, 1415–1431.
Jiménez, M.J., García-Fernández, M., Romero, J., 2008. 1989–1995 earthquake sequences in the Galeras volcano region, SW Colombia, and possible volcano–earthquake interactions. Tectonophysics 463, 47–59.
Johnson, D.J., Eggers, A.A., Bagnardi, M., Battaglia, M., Poland, M.P., Miklius, A., 2010. Shallow magma accumulation at Kilauea Volcano, Hawai'i, revealed by microgravity surveys. Geology 38, 1139–1142. doi:10.1130/G31323.1.
Jónsson, S., Segall, P., Pedersen, R., Björnsson, G., 2003. Post-earthquake ground movements correlated to pore-pressure transients. Nature 424, 179–183.
KWare, 1999. KWare magma — Geological software developed by Ken Wohletz [online]. Available: http://geodynamics.lanl.gov/Wohletz/Magma.htm. Last accessed 1 February 2011.
Lacruz, J., Ugalde, A., Vargas, C.A., Carcole, E., 2009. Coda-wave attenuation imaging of Galeras Volcano, Colombia. Bull. Seismol. Soc. Am. 99 (6), 3510–3515.
Lewicki, J.L., Fischer, T., Williams, S.N., 2000. Chemical and isotopic compositions of fluids at Cumbal Volcano, Colombia: evidence for magmatic contribution. Bull. Volcanol. 62, 347–361. doi:10.1007/s004450000100.
Loboguerrero, A., Gilboa, Y., 1987. Groundwater in Colombia. Hydrol. Sci. J. 32 (2), 161–178.
Londoño, J.M., Ospina, L.F., 2008. Estructura tridimensional de velocidad de onda P para el volcán Galeras. Bol. Geol. 42 (1–2), 7–23.
Lu, Z., Dzurisin, D., 2010. Ground surface deformation patterns, magma supply, and magma storage at Okmok volcano, Alaska, from InSAR analysis: 2. Coeruptive deflation, July–August 2008. J. Geophys. Res. 115, B00B03. doi:10.1029/2009JB006970.
Massonnet, D., Feigl, K.L., 1995. Satellite radar interferometric map of the coseismic deformation field of the M = 6.1 Eureka Valley, California earthquake of May 17, 1993. Geophys. Res. Lett. 22 (12), 1541–1544.
Masterlark, T., Haney, M., Dickinson, H., Fournier, T., Searcy, C., 2010. Rheologic and structural controls on the deformation of Okmok volcano, Alaska: FEMs, InSAR and ambient seismic noise tomography. J. Geophys. Res. 115, B02409. doi:10.1029/2009JB006324.
Melnik, O., Sparks, R.S.J., 2005. Controls on conduit magma flow dynamics during lava dome building eruptions. J. Geophys. Res. 110, 1–21. doi:10.1029/2004JB003183.
Mogi, K., 1958. Relations between the eruptions of various volcanoes and the deformations of the ground surfaces around them. Bull. Earthq. Res. Inst. Univ. Tokyo 36, 99–134.
Moran, S.C., Kwoun, O., Masterlark, T., Lu, Z., 2006. On the absence of InSAR-detected volcano deformation spanning the 1995–1996 and 1999 eruptions of Shishaldin Volcano, Alaska. J. Volcanol. Geoth. Res. 150, 119–131.
Murcia, H.F., Sheridan, M.F., Macías, J.L., Cortés, G.P., 2010. TITAN2D simulations of pyroclastic flows at Cerro Machín Volcano, Colombia: hazard implications. J. S. Am. Earth Sci. 29, 161–170.
Naranjo, J.L., Siggurdsson, H., Carey, S.N., Fritz, W., 1986. Eruption of the Nevado del Ruiz Volcano, Colombia, on 13 November 1985: tephra fall and lahars. Science 233, 991–993.
Narváez, L., Torres, R., Gómez, D., Cortés, G., Cepeda, H., Stix, J., 1997. Tornillo-type seismic signals at Galeras Volcano, Colombia, 1992–1993. J. Volcanol. Geotherm. Res. 77, 159–171.
Okada, Y., 1985. Surface deformation due to shear and tensile faults in a half-space. Bull. Seismol. Soc. Am. 75, 1135–1154.
Ordóñez, V.M.I., Rey, G.C.A., 1997. Deformation associated with the extrusion of a dome at Galeras volcano, 1990–1991. J. Volcanol. Geotherm. Res. 77, 115–120.
Pedersen, R., Sigmundsson, F., 2006. Temporal development of the 1999 intrusive episode in the Eyjafjallajökull volcano, Iceland, derived from InSAR images. Bull. Volcanol. 68, 377–393.
Pritchard, M.E., Simons, M., 2004. An InSAR-based survey of volcanic deformation in the central Andes. Geochem. Geophys. Geosyst. 5, Q02002. doi:10.1029/2003GC000610.
Pulgarín, B., Correa, A., Cepeda, H., Ancochea, E., 2001. Aspectos Geológicos del Complejo Volcánico Nevado del Huila. Memorias VIII Congreso Colombiano de Geología (Formato Digital), Manizales. 15 pp.
Rosen, P.A., Hensley, S., Peltzer, G., Simons, M., 2004. Updated repeat orbit interferometry package released. EOS Trans. Am. Geophys. Union 85 (4), 47.
Rymer, H., 1994. Microgravity change as a precursor to volcanic activity. J. Volcanol. Geotherm. Res. 61, 311–328.
Rymer, H., Cassidy, J., Locke, C.A., Murray, J.B., 1995. Magma movements in Etna volcano associated with the major 1991–1993 lava eruption: evidence from gravity and deformation. Bull. Volcanol. 57, 451–461.
Segall, P., 2010. Earthquake and Volcano Deformation. Princeton University Press, Princeton, N.J.
Seidl, D., Hellweg, M., Calvache, V.M.L., Gómez, D., Ortega, A., Torres, C.R., Böker, F., Buttkus, B., Faber, E., Greinwald, S., 2003. The multiparameter station at Galeras Volcano (Colombia): concept and realization. J. Volcanol. Geoth. Res. 125, 1–12.
Sigmundsson, F., Hreinsdottir, S., Hooper, A., Arnadottir, T., Pedersen, R., Roberts, M.J., Oskarsson, N., Auriac, A., Decriem, J., Einarsson, P., Geirsson, H., Hensch, M., Ofeigsson, B.G., Sturkell, E., Sveinbjornsson, H., Feigl, K., 2010. Intrusion triggering of the 2010 Eyjafjallajokull explosive eruption. Nature 468 (7322), 426-U253.
Stern, C.R., 2004. Active Andean volcanism: its geologic and tectonic setting. Rev. Geol. Chile 31 (2), 161–206.
Stix, J., Torres, C.R., Narvaez, M.L., Cortés, J.G.P., Raigosa, A.J., Gomez, M.D., Castonguay, R., 1997. A model of Vulcanian eruptions at Galeras volcano, Colombia. J. Volcanol. Geoth. Res. 77, 285–303.

Thouret, J.C., Cantagrel, J-M., Robin, C., Murcia, A., Salinas, R., Cepeda, H., 1995. Quaternary eruptive history and hazard-zone model at Nevado del Tolima and Cerro Machín Volcanoes, Colombia. J. Volcanol. Geoth. Res. 66, 397–426.

Trenkamp, R., Kellogg, J.N., Freymuller, J.T., Mora, H.P., 2002. Wide plate margin deformation, South Central America and Northwestern South America, CASA GPS observations. J. S. Am. Earth Sci. 15, 157–171.

Williams, S.N. (Ed.), 1990a. Nevado del Ruiz Volcano, Colombia, I: J. Volcan. Geotherm. Res., 41 (Special Issue).

Williams, S.N. (Ed.), 1990b. Nevado del Ruiz Volcano, Colombia, II: J. Volcan. Geotherm. Res., 42 (Special Issue).

Williams, C.A., Wadge, G., 1998. The effects of topography on magma chamber deformation models: application to Mt. Etna and radar interferometry. Geophys. Res. Lett. 25 (10), 1549–1552.

Williams, S.N., Calvache, V.M.L., Sturchio, N.C., Zapata, G.J.A., Mendez, F.R.A., Calvache, O.B., Londoño, C.A., Gil, C.F., Sano, Y., 1990. Premonitory geochemical evidence of magmatic reactivation of Galeras volcano, Colombia. EOS Trans. AGU 74 (43), 690.

Wright, T.J., Parsons, B.E., Jackson, J.A., Haynes, M., Fielding, E.J., England, P.C., Clarke, P.J., 1999. Source parameters of the 1 October 1995 Dinar (Turkey) earthquake from SAR interferometry and seismic bodywave modelling Oct. Earth Planet. Sci. Lett. 172, 23–37.

Wright, T.J., Lu, Z., Wicks, C., 2003. Source model for the M-w 6.7, 23 October 2002, Nenana Mountain Earthquake (Alaska) from InSAR. Geophys. Res. Lett. 30 (18). doi:10.1029/2003GL018014.

Zapata, G.J.A., Calvache, V.M.L., Cortés, J.G.P., Fischer, T.P., Garzon, V.G., Gómez, M.D., Narváez Medina, M.L., Ordóñez, V.M., Ortega, E.A., Stix, J., Torres, C.R., Williams, S.N., 1997. SO2 fluxes from Galeras Volcano, Colombia, 1989–1995: progressive degassing and conduit obstruction of a decade volcano. J. Volcanol. Geoth. Res. 77, 195–208.

Zebker, H.A., Amelung, F., Jonsson, S., 2000. Remote sensing of volcano surface and internal processes using radar interferometry. AGU Geophys. Monogr. 116, 179–205.